CMV Infection of Human Sinusoidal Endothelium Regulates Hepatic T Cell Recruitment and Activation

Bruns, Tony; Zimmermann, Henning W; Pachnio, Annette; Li, Ka-Kit; Trivedi, Palak J; Reynolds, Gary; Hubscher, Stefan; Stamataki, Zania; Badenhorst, Paul; Weston, Christopher J; Moss, Paul A; Adams, David H

DOI:
10.1016/j.jhep.2015.02.046

Accepted Manuscript

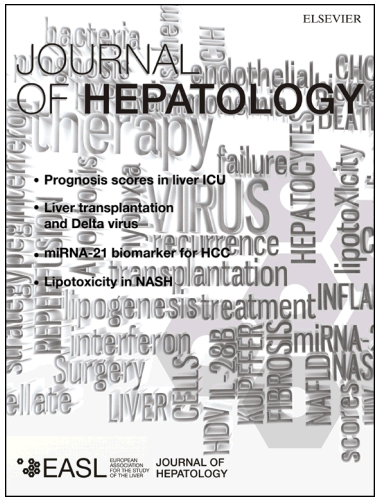

CMV Infection of Human Sinusoidal Endothelium Regulates Hepatic T Cell Recruitment and Activation

Tony Bruns, Henning W. Zimmermann, Annette Pachnio, Ka-Kit Li, Palak J. Trivedi, Gary Reynolds, Stefan Hubscher, Zania Stamataki, Paul W. Badenhors, Christopher J. Weston, Paul A. Moss, David H. Adams

PII: S0168-8278(15)00168-3
DOI: http://dx.doi.org/10.1016/j.jhep.2015.02.046
Reference: JHEPAT 5600

To appear in: *Journal of Hepatology*

Received Date: 11 December 2014
Revised Date: 16 February 2015
Accepted Date: 18 February 2015

Please cite this article as: Bruns, T., Zimmermann, H.W., Pachnio, A., Li, K-K., Trivedi, P.J., Reynolds, G., Hubscher, S., Stamataki, Z., Badenhors, P.W., Weston, C.J., Moss, P.A., Adams, D.H., CMV Infection of Human Sinusoidal Endothelium Regulates Hepatic T Cell Recruitment and Activation, *Journal of Hepatology* (2015), doi: http://dx.doi.org/10.1016/j.jhep.2015.02.046

Resubmission of Manuscript no. JHEPAT-D-14-02440R1

Title:

CMV Infection of Human Sinusoidal Endothelium Regulates Hepatic T Cell Recruitment and Activation

Authors:

1. Tony Bruns (1, 2, 3) tony.bruns@med.uni-jena.de
2. Henning W. Zimmermann (1, 4) henzimmermann@ukaachen.de
3. Annette Pachnio (5) a.pachnio@bham.ac.uk
4. Ka-Kit Li (1) kkl5@doctors.org.uk
5. Palak J. Trivedi (1) p.j.trivedi@bham.ac.uk
6. Gary Reynolds (1, 6) g.m.reynolds@bham.ac.uk
7. Stefan Hubscher (1, 6) s.g.hubscher@bham.ac.uk
8. Zania Stamataki (1) z.stamataki@bham.ac.uk
9. Paul W. Badenhorst (7) p.w.badenhorst@bham.ac.uk
10. Christopher J. Weston (1) c.j.weston@bham.ac.uk
11. Paul A. Moss (5) p.moss@bham.ac.uk
12. David H. Adams (1) d.h.adams@bham.ac.uk

Affiliations:

1. NIHR Biomedical Research Unit and Centre for Liver Research, University of Birmingham, Birmingham, United Kingdom
2. Department of Internal Medicine IV, Jena University Hospital, Friedrich Schiller University of Jena, Jena, Germany

3. Center for Sepsis Control and Care, Jena University Hospital, Friedrich Schiller University of Jena, Jena, Germany
4. Department of Medicine III, University Hospital Aachen, RWTH Aachen University, Aachen, Germany
5. School of Cancer Sciences, University of Birmingham, Birmingham, United Kingdom
6. Department of Cellular Pathology, Queen Elizabeth Hospital Birmingham, Birmingham, UK
7. School of Immunity and Infection, University of Birmingham, Birmingham, UK

Corresponding authors:

1. David H. Adams, MD, FRCP, FMedSci, Centre for Liver Research, 5th Floor IBR, College of Medical and Dental Sciences, Medical School Building, University of Birmingham, Edgbaston, Birmingham, B15 2TT, UK. Telephone +44 (0)121 415 8702. Email: d.h.adams@bham.ac.uk
2. Tony Bruns, MD, Department of Internal Medicine IV (Gastroenterology, Hepatology, Infectious Disease), Jena University Hospital, Erlanger Allee 101, 07740 Jena, Germany. Telephone +49 (0) 3 641 9 322 303. Telefax: +49 (0) 3 641 9 324 222. Email: tony.bruns@med.uni-jena.de

Electronic word count:

Figures:	7
Tables:	0
Abstract word count:	199/**250**
Manuscript word count (incl. abstract, figure legends, references):	5990/**6000**
Supplementary figures:	7

Conflict of interest:

The authors have no conflicting financial interests.

Financial support:

Tony Bruns was supported by the German Research Foundation (DFG BR4182/1-1) and receives support from the German Federal Ministry of Education and Research (BMBF, 01 E0 1002).

Authors' contributions:

Study concept and design: TB, PAM, DHA

Acquisition of data: TB, HWZ, AP, KKL, GMR, PWB

Analysis and interpretation of data: TB, SGH, PWB, PAM, DHA

Drafting of the manuscript: TB, DHA

Critical revision of the manuscript for important intellectual content: TB, HWZ, AP, KKL, PJT, GMR, SGH, ZS, PWB, CJW, PAM, DHA

Statistical analysis: TB, PWB

Technical or material support: AP, KKL, PJT, GMR, ZS, PWB, CJW, PAM, DHA

Study supervision: DHA

Acknowledgements:

We thank the staff at the Liver Transplant Unit, Queen Elizabeth Hospital Birmingham, UK for their help with sample collection and the patients for donating blood and tissue. We also thank Gill Muirhead and Janine Youster for their help with HSEC isolation and culture, Stephen Kissane for performing SAGE analysis, Richard Stanton for providing recombinant HCMV, and Sukhdeep Galsinh for measuring type-I interferons.

Key words:

Liver Immunology; Cytomegalovirus; Liver Sinusoidal Endothelial Cells; Transendothelial Migration

Abbreviations used:

BAC	bacterial artificial chromosome
CLEVER-1	common lymphatic endothelial and vascular endothelial receptor-1
EC	endothelial cells
ECM	endothelial cell medium
EPCR	endothelial protein C receptor
ETM	endothelial transmigration
FI	fluorescence intensity
Foxp3	forkhead box P3
HCMV	human cytomegalovirus
HFFF2	human fetal foreskin fibroblasts
HSEC	hepatic sinusoidal endothelial cells
ICAM-1	intercellular adhesion molecule-1
IMC	isotype-matched control
LCL	lymphoblastoid cell lines
LFA-3	lymphocyte function-associated antigen 3
MBCD	methyl-β-cyclodextrin
MCVM	murine cytomegalovirus
MOI	multiplicity of infection
p.i.	post infection
SAGE	serial analysis of gene expression
T_{EM}	effector memory T cells
Treg	regulatory T cells
VAP-1	vascular adhesion protein-1
VCAM-1	vascular cell adhesion molecule-1

BACKGROUND & AIMS: Human cytomegalovirus infection (HCMV) is associated with an increased morbidity after liver transplantation by facilitating allograft rejection and accelerating underlying hepatic inflammation. We hypothesized that human hepatic sinusoidal endothelial cells infected with HCMV possess the capacity to modulate allogeneic T cell recruitment and activation thereby providing a plausible mechanism of how HCMV infection is able to enhance hepatic immune activation.

METHODS: Human hepatic sinusoidal endothelial cells were isolated from explanted livers and infected with recombinant endotheliotropic HCMV. We used static and flow-based models to quantify adhesion and transendothelial migration of allogeneic T cell subsets and determine their post-migratory phenotype and function.

RESULTS: HCMV infection of primary human hepatic sinusoidal endothelial cells facilitated ICAM-1 and CXCL10-dependent CD4 T cell transendothelial migration under physiological levels of shear stress. Recruited T cells were primarily non-virus-specific CXCR3^{hi} effector memory T cells, which demonstrated features of LFA3-dependent Th1 activation after migration. In parallel, regulatory T cells were more strongly recruited via infected hepatic endothelium and retained a suppressive phenotype following transmigration.

CONCLUSIONS: The ability of infected hepatic endothelium to recruit distinct functional CD4 T cell subsets shows how HCMV facilitates hepatic inflammation and immune activation and may simultaneously favor virus persistence.

Introduction

Hepatic sinusoidal endothelial cells (HSEC) differ from endothelial cells (EC) in other vascular beds. Leukocytes entering the liver through the sinusoids undergo sequential interactions with HSECs, which are selectin-independent and involve non-classical adhesion molecules[1, 2]. In addition, HSEC are capable of presenting and cross-presenting exogenous antigen to CD4 and CD8 T cells thereby contributing to local immune regulation in the liver[3, 4]. As a scavenger cell population, HSEC also bind and capture circulating hepatotropic viruses to facilitate infection of hepatocytes[5–7]. Human cytomegalovirus (HCMV) is a ubiquitous herpes virus that persists for the life of the host after initial infection and infects many cell types including epithelial, mesenchymal, and EC during acute infection[8].

The liver represents a major target leading to virus-induced hepatitis and liver cell damage in immunocompetent and immunocompromised hosts. Hepatocytes are permissive for cytomegalovirus infection *in vivo* and *in vitro*[9], but hepatocyte-derived murine CMV (MCMV) fails to leave the liver but infects adjacent EC[10, 11]. Although it has long been recognized that EC in many organs are capable of harboring viral DNA during CMV latency[12], sinusoidal EC have only recently been identified as the source of MCMV latency and reactivation within the liver[13]. Consistent with this previous studies report that HCMV infection of HSEC frequently precedes hepatocyte infection in liver allograft recipients[14]. In the organ transplant setting HCMV infection of the seronegative recipient is associated with an increased risk of graft-loss and death after liver transplantation[15] and HCMV infection can promote hepatic inflammation and facilitate chronic organ rejection[16]. The molecular basis of this observation is not clear, but MCMV infection of murine HSEC activates a gene expression pattern associated with increased expression of

chemokines and adhesion molecules and the promotion of an immunogenic CD8 T cell response[17].

We hypothesized that HCMV infection will modulate the ability of human HSEC to recruit and activate effector T cells thereby providing a mechanism to explain how HCMV infection increases hepatic immune activation in allograft rejection.

Materials and Methods

Human tissue and blood

Liver tissue obtained from explanted livers or tissue surplus to surgical requirements was collected from patients in the Liver Unit at the Queen Elizabeth Hospital (Birmingham, UK) with informed consent. HSEC were isolated from liver tissue and cultured as previously reported[2]. PBMC were isolated from healthy donor blood by density gradient centrifugation and T cell subsets were isolated using immunomagnetic separation or flow cytometry cell sorting. For indicated experiments, HCMV-reactive CD4 T cells were generated from CMV-seropositive donors using cell cloning by limiting dilution as described in the Supplementary Materials and Methods section.

Recombinant human CMV

To study endothelial HCMV infection we used the bacterial artificial chromosome (BAC)-cloned strain recombinant CMV1426 (from BAC pAL1426), which was a gift from Richard Stanton. CMV1426 contains an internal ribosomal entry site, followed by enhanced green fluorescent protein (EGFP) after UL122, a frame shift mutation in RL13[18], and the UL128 locus derived from endotheliotropic TB40-BAC4[19]. CMV1426 was propagated and purified as described in the Supplementary Materials

and Methods section. Virus was then titrated to maintain an intact EC monolayer using 0.1–0.3 multiplicity of infection (MOI) after spinfection (20 min, 800×*g*) and further 100 min of virus incubation in serum-free medium followed by rigorous washing to remove unbound virus.

Flow-based adhesion and migration

Lymphocyte interaction with confluent monolayers of HSEC was assessed in flow-based adhesion assays at physiological shear stress as previously described[20]. HSEC monolayers were either CMV1426-infected or mock-infected and cultivated for subsequent 24 hours, and remained untreated or stimulated with combinations of recombinant TNF-α, IFN-γ, IFN-α, or IFN-β at 10 ng/ml for 24 hours (PeproTech, Peterborough, UK). PBL or purified T cell subsets were flowed over HSEC monolayers for 5 min followed by a washout phase of another 5 min. Cells appearing bright in phase contrast microscopy were above the endothelial monolayer, whereas those that were dark had migrated. To determine the molecular bases of the interactions, HSEC monolayers and/or lymphocytes were incubated with blocking Abs for 30 min in individual experiments as indicated and the respective isotype-matched controls (IMC) (see the Supplementary Materials and Methods section).

Static migration

HSEC were grown until confluence in collagen-coated plates, CMV1426-infected or mock-infected, detached, and reseeded either on either collagen-coated cell culture transwell inserts with 3-µm pore size (BD Biosciences, Oxford, UK) for short-term transwell experiments or fibronectin-coated polymerized bovine collagen I plugs (Gibco, Life Technologies, Paisley, UK) for long-term experiments. In the transwell model T cells allowed to migrate across HCMV-infected or cytokine-stimulated HSEC

to the bottom chamber within 4 hours. In the collagen model T cells were allowed to adhere to HCMV-infected or mock-infected HSEC for 2 hours, and migrate over 24-48 hours into collagen. Migrated cells were retrieved using collagenase digestion and used in flow cytometry or functional assays as described in the Supplementary Materials and Methods section.

Cytokine secretion

Cytokines and chemokines released into the supernatant were quantified using ELISArray Kits (SABioscience/Qiagen, West Sussex, UK), ISG56-Luciferase reporter transfected Huh-7.5 cells, or the proteome profiler kit (R&D Systems, Abingdon, UK) as described in the Supplementary Materials and Methods section.

T cell suppression

Migrated CD4 T cells were co-cultured with CellTrace violet-labeled (Life Technologies) responder T cells from healthy donors in varying ratios in the presence of CD3/CD28 activating beads (Treg inspector; Miltenyi Biotec). Flow cytometry was carried out to determine responder cell division after 3 days (see Supplementary Materials and Methods section).

Gene expression

Serial analysis of gene expression (SAGE) was performed 24 hours after mock infection, cytokine stimulation with TNF-α and IFN-γ at 10 ng/ml, or infection with CMV1426 (MOI 0.3) in isolated HSEC from patients with autoimmune hepatitis, seronegative hepatitis, and alcoholic liver disease as described in the Supplementary Materials and Methods section. Modulated gene expression in CD4 memory T cells before and after endothelial transmigration (ETM) through CMV-infected HSEC was

determined using the RT^2 Profiler PCR Array Human T Helper Cell Differentiation Kit (SABiosciences/Qiagen) (see Supplementary Materials and Methods).

Multicolor confocal microscopy

Live-cell immunofluorescence staining of CMV1426-infected or mock-infected HSEC for ICAM-1 and LFA-3 was performed on an upright 780 ZEN laser scanning confocal microscope (Zeiss, Oberkochen, Germany) as described in the Supplementary Materials and Methods section.

Statistical analysis

Statistical tests were performed using Prism 5.0 software (GraphPad, La Jolla, CA). Results are expressed as mean and standard error of mean unless otherwise stated. Two-tailed Student's t test or ANOVA with post-hoc Dunnett's multiple comparison tests were used to determine the significance of differences between groups as appropriate. *P* values less than .05 were considered significant.

Results

HSEC are permissive for HCMV infection

Infection of primary HSEC with CMV1426 (MOI 0.1-0.3) resulted in the typical cytopathic effect beginning at 24 hours post infection (p.i.) (**Figure 1A**). EGFP expression was seen in enlarged rounded cells and spread in culture for up to 12-14 days before the monolayer was destroyed and infected cells lifted off (**Figure 1B**). Supernatant from infected HSEC was infective after a delay of 2 days resulting in stable HCMV concentrations in the supernatant after 6 days that were able to infect human fetal foreskin fibroblasts (HFFF2) (**Figure 1C**).

Liver sinusoidal HCMV infection induces a distinct regulation of cell adhesion molecules and chemokines

Serial analysis of gene expression (SAGE) in mock- and HCMV-infected HSEC revealed that among the 141 differentially regulated genes the vast majority (120) was significantly downregulated after HCMV infection. This was in sharp contrast to endothelium treated with TNF-α and IFN-γ[2], where the upregulation of gene expression dominated (**Supplementary Figure S1**). Analysis of the regulation of a pre-selected panel of mRNAs revealed varying upregulation of intercellular adhesion molecule-1 (ICAM-1) and the chemokines CXCL8, CXCL9, CXCL10, and CX3CL1 following HCMV infection in at least two of three liver donors 24 hours p.i. (**Figure 2A**).

In addition to CXCR3 ligands, murine genes encoding CCR5 ligands (*Ccl4*, *Ccl5*) have been shown to be significantly upregulated in a model of CMV infection of liver sinusoidal EC[17]. Therefore we measured the release of the respective human chemokines in HSEC supernatants after HCMV infection. Among those, CXCL10 secretion was significantly elevated following HCMV infection exceeding 1000-fold the concentrations measured for mock-infected HSEC 24 hours p.i. (**Figure 2B**). CXCL10 release from HSEC was dose-dependent, fell to control levels during the viral eclipse phase, and was released during viral spread with similar kinetics to CXCL8 and IL-6 (**Supplementary Figure S2**). Consistent with reports that ligands of CXCR3, CCR5, and CX3CR1 can be induced by type I interferons in microvascular endothelium from other organs[21], we measured a significant release of type I interferons by HSEC following HCMV infection contributing to chemokine induction (**Figure 2C**).

To investigate surface cell adhesion molecule expression following replicative HCMV infection we used flow cytometry gating on EGFP-positive HCMV-infected HSEC compared to mock-infected HSEC and cytokine-stimulated HSEC known to optimally promote lymphocyte adhesion and ETM as a positive control[2]. Cultured HSEC expressed detectable levels of intercellular adhesion molecule (ICAM)-1, ICAM-2, and lymphocyte function-associated antigen 3 (LFA-3) in the absence of exogenous cytokine stimulation but no expression of vascular cell adhesion molecule-1 (VCAM-1) or E-selectin and cytokine treatment strongly increased expression of VCAM-1 and ICAM-1. Following HCMV infection, there was a significant increase in ICAM-1 expression, but no induction of VCAM-1, ICAM-2, E-Selectin or vascular adhesion protein-1 (VAP-1) (**Figure 2D and E)**. Confocal microscopy of live HCMV-infected HSEC monolayers confirmed an increased ICAM-1 expression on infected HSEC with LFA-3 enrichment at intercellular junctions (**Figure 2F**).

Viral replication was required for ICAM-1 and CXCL10 induction, which were abrogated when UV-irradiated virus was used (**Figure 2B**) or if cells demonstrated no viral replication (**Figure 2D, Supplementary Figure 3A**). Accordingly, treatment of HSEC with UV-inactivated virus did not result in a significantly increased adherence of PBMC to endothelium under flow (**Supplementary Figure 3B**).

Liver sinusoidal HCMV infection promotes adhesion and migration of T cell subsets under flow

We went on to investigate the functional consequences of HCMV infection for lymphocyte ETM under conditions of physiological shear stress[2]. When HSEC were infected with HCMV maintaining an intact monolayer at 24 hours p.i. freshly isolated allogeneic PBL bound in greater numbers to HCMV-infected endothelium compared to mock-infected endothelium and showed increased rates of ETM (**Figure 3A**)**.** TNF-

α/IFN-γ-treated HSEC supported increased adhesion and migration and in some experiments this was further increased by prior HCMV infection. In contradistinction, treatment with IFN-α/IFN-β at doses of 10 ng/ml each did not alter the total number of adherent and migrating PBL (**Figure 3B**) consistent with a lack of upregulation of ICAM-1 following type I interferon treatment (**Supplementary Figure S4**).

A similar response was seen when the experiments were repeated using highly pure CD4 T cells isolated from blood. Blocking antibodies against ICAM-1 significantly reduced absolute adherence and migration, whereas VAP-1 and common lymphatic endothelial and vascular endothelial receptor-1 (CLEVER-1) blocking antibodies did not show a significant effect (**Figure 3C**). Treatment with anti-CXCL10 antibodies did not reduce the absolute number of migrating T cells but did reduce the percentage of adherent cells undergoing ETM (**Figure 3D**).

CMV-specific CD4 T cell clones, which secreted IFN-γ in response to autologous CMV peptide-pulsed EBV–transformed lymphoblastoid cell lines (LCL) and displayed an activated effector phenotype (CD45RO^{+}CD62L^{-}CD2^{hi}CD11a^{hi}CD18^{hi}), bound to and migrated at 5 times greater numbers than resting CD4 T cells. HCMV infection of HSEC resulted in an increased number of cells adhering and migrating, which could be abrogated using an anti-ICAM-1 blocking antibody on endothelium (**Figure 3E**). In addition, expanded polyclonal CD4 CD25^{hi} Treg also bound to HCMV-infected HSEC although at lower frequencies than the CD4 clones. Their adhesion and transmigration was reduced by approximately 50% by blocking ICAM-1 (**Figure 3F**) supporting the role of ICAM-1 as a predominant mechanism promoting adhesion to and migration across HCMV-infected HSEC in all investigated T cell subsets.

Effector memory T cells expressing CXCR3 and CCR5 predominantly migrate across HSEC

To investigate changes in the T cell phenotype after ETM, we employed two static models. In the first model lymphocytes migrated across HSEC into collagen and remained subendothelial for 24 to 72 hours allowing us to study differentiation after migration; in the second model lymphocytes migrated across HSEC seeded onto collagen-coated 3 µm transwell filters allowing us to study early recruitment (**Figure 4A**). In both models there were no significant differences in the distribution of migrated CD4, CD8, γδ T cells, and NKT cells between mock- and HCMV-infected HSEC in the collagen model or between cytokine-stimulated and HCMV-infected HSEC in the transwell model (**Figure 4B**).

After migration through cytokine-treated and HCMV-infected HSEC in the transwell model, T cell populations expressing CXCR3 and/or CCR5 were increased compared to the pre-migratory cell population (**Figure 3C**). In addition, migrated T cells had higher surface expression of the LFA-3 ligand CD2 and the ICAM-1 ligand CD11a/CD18 (LFA-1, $\alpha_L\beta_2$ integrin) (**Figure 3D**). To further dissect the phenotype of CD4 T cells migrating through infected HSEC with respect to their homing and effector functions, we stained migrating CD4 T cells for the memory marker CD45RO and two lymphocyte homing receptors CD62L and CCR7. While CD4 T cells adherent to infected endothelium did not show any difference in expression of CD45RO and CD62L compared to the starting population of purified CD4 T cells, T cells that migrated across HCMV-infected endothelium where predominantly CD45RO-positive memory T cells with reduced CD62L expression (**Figure 4E**). $CD62L^-CCR7^-$ effector memory T cells (T_{EM}) were selectively enriched after migration through HSEC with the highest fraction being observed after migration through

HCMV-infected HSEC (**Figure 4F**). To estimate whether HCMV-reactive T cells from seropositive donors were also enriched following migration of PBMC across HCMV-infected HSEC we determined CD4 T cell activation in response to HCMV lysate by measuring de-novo synthesized CD154 [22]. An increased number of reactive T cells were observed migrating across infected HSEC when compared to mock-infected or cytokine stimulated endothelium but this population was not enriched for HCMV-responding T cells. This suggests that the vast majority of migrating effector T cells were not HCMV-reactive (**Supplementary Figure S5**).

Transmigration through HCMV-infected HSEC induces cell contact-dependent Th1 activation of memory CD4 cells

Based on our observations of increased adhesion and migration of T_{EM} through HCMV-infected HSEC, we used purified allogeneic $CD45RO^+$ CD4 memory T cells from CMV-positive and CMV-negative donors to study T cell activation after ETM because immunohistochemical staining of liver biopsies suggested an increased level of activated T cells within the CMV-infected liver (**Supplementary Figure S6**). Using the described *in vitro* models of T cell migration through a monolayer of endothelium, twenty-four to 48 hours after migration through HCMV-infected HSEC, CD4 memory T cells displayed increased expression of the activation markers CD69, CD71, CD25, and HLA-DR compared to pre-migratory T cells (**Figure 5A and B**). Upregulation of activation markers after transmigration occurred irrespective of T cell donor's CMV serostatus and was not observed after migration across mock-infected or cytokine-stimulated endothelium (**Supplementary Figure S7**). CD69+ CD4 T cells that had migrated through HCMV-infected endothelium showed increased spontaneous IFN-γ secretion without further stimulation but no increase in intracellular TNF-α or IL-10 (**Figure 5C**), and supernatant derived from migrated CD4

memory cells contained detectable levels of IFN-γ and soluble CD154 (**Figure 5D**). After stimulation with PMA and ionomycin the cells secreted high levels of IL-2, TNF-α and GMCSF but no detectable Th2 or Th17 cytokines (**Figure 5D**). After migration through HCMV-infected HSEC *IFNG* gene expression was strongly upregulated together with other components of Th1-differentiated CD4 T cells including the signal transducer and activator of transcription 1 (*STAT1*), the key regulator of Th1 differentiation and driver of IFN-γ production T-bet (*TBX21*) and the IL-12 receptor (*IL12RB2)* (**Figure 5E**). This activation programme depended on cell-cell contact and did not occur when HSEC and memory T cells were separated by a non-cell permeable filter of 0.3 µm excluding activation by soluble factors (**Figure 5F**). Blocking the LFA-3/CD2 pathway by incubating HSEC with mAbs against LFA-3 resulted in a 29% decrease of CD69 expressing migrated memory T cells whereas blocking mAbs against ICAM-1, CXCL10, TLR2, endothelial protein C receptor, inhibiting the JAK-STAT signaling pathway in infected HSEC (EPCR), or removing cholesterol from lipid rafts by methyl-β-cyclodextrin (MBCD) had no effect on T cell activation post migration (**Figure 5F**).

HCMV-infected endothelium recruits functional regulatory T cells

In keeping with our earlier observation that CD4 Treg showed increased migration across infected versus non-infected HSEC in flow-based adhesion assays, we found that genes associated with Treg differentiation, forkhead box P3 (*FOXP3*) and IL-2 receptor alpha (*IL2RA*), were upregulated after migration through HCMV-infected endothelium (**Figure 5E**). This suggests that the enrichment of $CD25^{hi}$ CD4 T cells after migration through HCMV-infected HSEC could be due to the recruitment and/or induction of Treg as well as activated effector cells.

The number of early and late apoptotic cells after migration through HCMV-infected and mock-infected HSEC into collagen did not change between 24 and 72 hours excluding induction of T cell apoptosis post migration (**Figure 6A**). A large proportion of migrated $CD25^{hi}$ CD4 T cells were $CD127^{lo}$ with FoxP3 expression, consistent with a regulatory T cell phenotype (**Figure 6B**). The frequency of $CD25^{hi}$ expressing CD4 T cells did not increase during incubation over time in the collagen model suggesting selective recruitment rather than proliferation (**Figure 6C**). Similar results were seen in the transwell model where HCMV-infected HSEC recruited a higher proportion of $CD127^{lo}CD25^{hi}$ $FoxP3^{+}$ memory T cells compared with cytokine-treated HSEC at early time-points (**Figure 6D**). As a consequence of the increased fraction of Treg, CD4 T cells were able to suppress T cell proliferation after migration through HCMV-infected endothelium when compared with T cells that migrated across cytokine-stimulated HSEC (**Figure 6E**).

Discussion

HSEC represent uniquely differentiated microvascular EC that play a critical role in regulating hepatic immune responses. They are responsible for regulating the recruitment of circulating lymphocytes into the hepatic parenchyma and also contribute to hepatic immune regulation through their ability to act as APCs that under the right conditions can induce both CD8 and CD4 T cell tolerance. These properties allow the liver to mount swift immune responses to infections such as hepatitis A whilst preventing immune activation to harmless food antigens entering via the gut.

Recent evidence from murine models suggests that sinusoidal endothelium is permissive to CMV infection and can act as a source of infection for adjacent

hepatocytes[10, 13]. MCMV infection of murine sinusoidal endothelium results in a switch from a tolerogenic to an immunogenic phenotype and promotes the ability of HSEC to induce full differentiation of cytotoxic effector CD8 T cells after cross-presentation thereby breaking an important tolerogenic mechanism[17]. The clinical significance of this finding is emphasized by the increased incidence of graft rejection in liver transplant recipients with CMV infection[15, 23]. Since CMV replication is species restricted and significant diversity exists between human and murine CMV, animal models cannot be relied upon to recapitulate the events that occur in patients during clinical CMV infection. In the present study we use *in vitro* models of primary human cells to demonstrate how HCMV infection of HSEC promotes adhesion and migration of allogeneic T cell subsets thereby leading to an enrichment of predominantly non-virus-specific Th1-differentiated CD4 T cells and functional Treg.

In contrast to hepatotropic viruses that do not replicate in HSEC[5–7], we show that inoculation of HSEC with live HCMV results in endothelial infection promoting hepatic T cell recruitment via upregulation of ICAM-1 surface expression and the release of chemokine ligands for the inflammatory chemokine receptors CXCR3 and CCR5 (**Figure 7**). Our findings are in line with histopathological studies describing increased ICAM-1 expression on liver endothelium in biopsies from CMV-infected liver transplants[24] and provide a mechanism by which sinusoidal EC regulate CXCR3-dependent accumulation of T cells in the murine model[25]. Importantly, the inflammatory endothelial phenotype induced by CMV infection promoting ETM differed from that seen in response to inflammatory cytokines suggesting that CMV infection has a specific effect on endothelial activation.

HCMV-infected HSEC preferentially recruited particular subsets of T cells. Memory CD4 T cells that were $CD45RO^{+}CCR7^{-}CD62L^{-}$, CXCR3, and/or CCR5 positive with high surface expression of CD2 and $\alpha_L\beta_2$ integrins were selectively enriched following ETM corresponding to the phenotype of T cells infiltrating inflamed tissues *in vivo*[26]. Furthermore these memory T cells were enriched for IFN-γ secreting Th1 cells and expressed markers of recent activation. This activation was not antigen-specific but in part dependent on adhesion through the LFA-3-CD2 pathway in an allogeneic context. Thus virally infected HCMV endothelium is able to promote the recruitment and differentiation of particular T cell subsets even if these cells are not antigen-specific.

In contrast to naïve CD4 T cells and central memory T cells, which must be activated in lymphoid organs before they develop an effector phenotype, HCMV-infected cells could activate polyclonal T cells to secrete Th1 cytokines immediately on recruitment into the liver. This is consistent with previous studies showing that IFN-γ secretion by CD4 T_{EM} in response to allogeneic EC is dependent on LFA-3 engagement but independent of CD80 and CD86 stimulation in co-culture models[27]. In our study adhesion to HCMV-infected HSEC alone was insufficient to induce significant T cell activation which required ETM. This mechanism could rapidly deliver IFN-γ secreting effector cells into the CMV-infected liver parenchyma. The clinical relevance of our study is supported by a large observational study showing the presence of similarly activated T cells in the hepatic parenchyma of CMV-infected allografts[24]. CD4 T_{EM} are important mediators of allograft rejection[27] suggesting that the recruitment and activation of alloreactive T_{EM} through HCMV-infected HSEC could explain how CMV infection can trigger allograft rejection.

Interestingly, we also observed an ICAM-1-dependent recruitment of functional Treg by HCMV-infected HSEC as a presumably important mechanism to counterbalance the pro-inflammatory CD4 T cell recruitment in an attempt to limit bystander tissue injury. The functional consequences of the increased T cell recruitment through CMV-infected HSEC may depend on the balance and kinetics of effector T cell versus Treg recruitment mediating liver allograft tolerance[28] but also promoting persistent viral infection[29]. Indeed, we have previously demonstrated that both Treg and effector T cells employ identical mechanisms, namely CXCR3/CXCR3-ligand and $\alpha_L\beta_2$/ICAM-1 interaction, in order to migrate across cytokine-stimulated hepatic endothelium[20,30].

In summary, we show for the first time how HCMV infection of sinusoidal endothelium modulates the recruitment and differentiation of T cell subsets using human primary cells. Despite the limitations of such *in vitro* models, our work has implications for how viral infection can modulate hepatic immunity, particularly in the context of liver transplantation. Further work is required to clarify how the critical balance of protective anti-viral effector T cells, potentially harmful non-specific effector T cells and tolerogenic regulatory T cells is controlled during hepatic HCMV-infection in the context of immunosuppression.

References

[1] Adams DH,Hubscher SG,Fisher NC,Williams A,Robinson M. Expression of E-selectin and E-selectin ligands in human liver inflammation. Hepatology 1996;24:533–8.

[2] **Shetty S,Bruns T,**Weston CJ,Stamataki Z,Oo YH,Long HM,et al. Recruitment mechanisms of primary and malignant B cells to the human liver. Hepatology 2012;56:1521–31.

[3] Knolle PA,Schmitt E,Jin S,Germann T,Duchmann R,Hegenbarth S,et al. Induction of cytokine production in naive CD4(+) T cells by antigen-presenting murine liver sinusoidal endothelial cells but failure to induce differentiation toward Th1 cells. Gastroenterology 1999;116:1428–40.

[4] Limmer A,Ohl J,Kurts C,Ljunggren H-G,Reiss Y,Groettrup M,et al. Efficient presentation of exogenous antigen by liver endothelial cells to CD8+ T cells results in antigen-specific T-cell tolerance. Nat Med 2000;6:1348–54.

[5] Breiner KM,Schaller H,Knolle PA. Endothelial cell-mediated uptake of a hepatitis B virus: a new concept of liver targeting of hepatotropic microorganisms. Hepatology 2001;34:803–8. doi:10.1053/jhep.2001.27810.

[6] Cormier EG,Durso RJ,Tsamis F,Boussemart L,Manix C,Olson WC,et al. L-SIGN (CD209L) and DC-SIGN (CD209) mediate transinfection of liver cells by hepatitis C virus. Proc Natl Acad Sci USA 2004;101:14067–72.

[7] Lai WK,Sun PJ,Zhang J,Jennings A,Lalor PF,Hubscher S,et al. Expression of DC-SIGN and DC-SIGNR on human sinusoidal endothelium: a role for capturing hepatitis C virus particles. Am J Pathol 2006;169:200–8.

[8] Sinzger C,Digel M,Jahn G. Cytomegalovirus cell tropism. Curr Top Microbiol Immunol 2008;325:63–83.

[9] Sinzger C,Bissinger AL,Viebahn R,Oettle H,Radke C,Schmidt CA,et al.

Hepatocytes Are Permissive for Human Cytomegalovirus Infection in Human Liver Cell Culture and in vivo. J Infect Dis 1999;180:976–86.

[10] Sacher T,Podlech J,Mohr CA,Jordan S,Ruzsics Z,Reddehase MJ,et al. The major virus-producing cell type during murine cytomegalovirus infection,the hepatocyte,is not the source of virus dissemination in the host. Cell Host Microbe 2008;3:263–72.

[11] Sacher T,Andrassy J,Kalnins A,Dölken L,Jordan S,Podlech J,et al. Shedding light on the elusive role of endothelial cells in cytomegalovirus dissemination. PLoS Pathog 2011;7:e1002366.

[12] Koffron AJ,Hummel M,Patterson BK,Yan S,Kaufman DB,Fryer JP,et al. Cellular localization of latent murine cytomegalovirus. J Virol 1998;72:95–103.

[13] Seckert CK,Renzaho A,Tervo H-M,Krause C,Deegen P,Kühnapfel B,et al. Liver Sinusoidal Endothelial Cells Are a Site of Murine Cytomegalovirus Latency and Reactivation. J Virol 2009;83:8869–84.

[14] Theise ND,Conn M,Thung SN. Localization of cytomegalovirus antigens in liver allografts over time. Hum Pathol 1993;24:103–8.

[15] Bosch W,Heckman MG,Diehl NN,Shalev JA,Pungpapong S,Hellinger WC. Association of cytomegalovirus infection and disease with death and graft loss after liver transplant in high-risk recipients. Am J Transplant 2011;11:2181–9.

[16] O'Grady JG,Alexander GJ,Sutherland S,Donaldson PT,Harvey F,Portmann B,et al. Cytomegalovirus infection and donor/recipient HLA antigens: interdependent co-factors in pathogenesis of vanishing bile-duct syndrome after liver transplantation. Lancet 1988;2:302–5.

[17] Kern M,Popov A,Scholz K,Schumak B,Djandji D,Limmer A,et al. Virally Infected Mouse Liver Endothelial Cells Trigger CD8+ T-Cell Immunity. Gastroenterology 2010;138:336–46.

[18] Stanton RJ,Baluchova K,Dargan DJ,Cunningham C,Sheehy O,Seirafian S,et al. Reconstruction of the complete human cytomegalovirus genome in a BAC reveals RL13 to be a potent inhibitor of replication. J Clin Invest 2010;120:3191–208.

[19] Sinzger C,Hahn G,Digel M,Katona R,Sampaio KL,Messerle M,et al. Cloning and sequencing of a highly productive,endotheliotropic virus strain derived from human cytomegalovirus TB40/E. J Gen Virol 2008;89:359–68.

[20] Shetty S,Weston CJ,Oo YH,Westerlund N,Stamataki Z,Youster J,et al. Common Lymphatic Endothelial and Vascular Endothelial Receptor-1 Mediates the Transmigration of Regulatory T Cells across Human Hepatic Sinusoidal Endothelium. J Immunol 2011;186:4147–55. doi:10.4049/jimmunol.1002961.

[21] Nakano M,Fujii T,Hashimoto M,Yukawa N,Yoshifuji H,Ohmura K,et al. Type I interferon induces CX3CL1 (fractalkine) and CCL5 (RANTES) production in human pulmonary vascular endothelial cells. Clin Exp Immunol 2012;170:94–100.

[22] Chattopadhyay PK,Yu J,Roederer M. Live-cell assay to detect antigen-specific CD4+ T-cell responses by CD154 expression. Nat Protoc 2006;1:1–6. doi:10.1038/nprot.2006.1.

[23] Evans PC,Soin A,Wreghitt TG,Taylor CJ,Wight DG,Alexander GJ. An association between cytomegalovirus infection and chronic rejection after liver transplantation. Transplantation 2000;69:30–5.

[24] Lautenschlager I,Halme L,Höckerstedt K,Krogerus L,Taskinen E. Cytomegalovirus infection of the liver transplant: virological,histological,immunological,and clinical observations. Transpl Infect Dis 2006;8:21–30.

[25] Hokeness KL,Deweerd ES,Munks MW,Lewis CA,Gladue RP,Salazar-Mather TP. CXCR3-Dependent Recruitment of Antigen-Specific T Lymphocytes to the Liver during Murine Cytomegalovirus Infection. J Virol 2007;81:1241–50.

[26] Qin S,Rottman JB,Myers P,Kassam N,Weinblatt M,Loetscher M,et al. The chemokine receptors CXCR3 and CCR5 mark subsets of T cells associated with certain inflammatory reactions. J Clin Invest 1998;101:746–54.

[27] Shiao SL,Kirkiles-Smith NC,Shepherd BR,McNiff JM,Carr EJ,Pober JS. Human effector memory CD4+ T cells directly recognize allogeneic endothelial cells in vitro and in vivo. J Immunol 2007;179:4397–404.

[28] Demirkiran A,Baan CC,Kok A,Metselaar HJ,Tilanus HW,van der Laan LJW. Intrahepatic detection of FOXP3 gene expression after liver transplantation using minimally invasive aspiration biopsy. Transplantation 2007;83:819–23.

[29] Li S,Gowans EJ,Chougnet C,Plebanski M,Dittmer U. Natural Regulatory T Cells and Persistent Viral Infection. J Virol 2008;82:21–30.

[30] Oo YH,Weston CJ,Lalor PF,Curbishley SM,Withers DR,Reynolds GM,et al. Distinct roles for CCR4 and CXCR3 in the recruitment and positioning of regulatory T cells in the inflamed human liver. J Immunol 2010;184:2886–98.

Figure legends

Figure 1: HSEC are permissive for HCMV infection.

(A) Morphology of mock-infected (top) and CMV1426-infected (bottom) HSEC monolayers 24 hours p.i. illustrating the cytopathic effect of HCMV. (B) EGFP expression demonstrating viral spread of HCMV 2-12 days p.i. in infected HSEC monolayers. (C) Representative one-step growth curve of supernatant HCMV infectivity in as determined by plaque assay on HFFF2 (circles) and increasing percentage of EGFP-positive HSEC (diamonds) as determined by flow cytometry.

Figure 2. HCMV infection regulates HSEC adhesion molecule expression and chemokine release

(A) Heat map showing normalized expression of human target genes of interest following infection of HSEC with CMV1426. (B) Chemokine concentrations in serum-containing conditioned supernatant HCMV-infection, mock-infection or inoculation with UV-irradiated HCMV (4-6 independent experiments, Dunnett's post hoc test). (C) Supernatant from HCMV-infected HSEC stimulates the type I IFN target gene ISG56 in Huh-7.5 hepatoma cells in a luciferase reporter assay (4 independent experiments, t test). (D) Representative flow cytometry plots of side scatter (SSC) and EGFP expression in HCMV-infected or mock-infected HSEC 7d p.i. showing increasing ICAM-1 surface expression in HSEC without (dotted), with moderate (grey), and with high (solid black) EGFP expression. (E) Surface molecule expression on mock-infected (white), EGFP-positive HCMV-infected (grey) and cytokine-treated (black) HSEC 24 hours p.i. as determined by flow cytometry (3-8 independent experiments, t test). (F) Representative confocal microscopy of HSEC monolayers after live surface staining for ICAM-1 (red) and LFA-3 (blue) in HCMV-infected and mock-infected HSEC.

Figure 3: HCMV-infected HSEC recruit T cells via ICAM-1 and CXCL-10 under flow

(A) Representative phase contrast microscopy video stills showing adherent non-migrating (white arrows) and migrating (black arrows) PBL to mock-infected, cytokine-treated and HCMV-infected HSEC. HCMV-infected HSEC with cytopathic effect are shown (arrow heads). (B) Quantification of adherent non-migrating and migrating allogeneic PBL in flow-based adhesion assays to mock-infected, type-I interferon-treated and HCMV-infected HSEC. TNF-α and IFN-γ-stimulated HSEC are shown as a positive control (at least 4 independent experiments, Dunnett's post hoc test of total cells adherent cells). (C) Adherent non-migrating and migrating allogeneic CD4 T cells after flow over mock-infected and HCMV-infected HSEC showing significant decrease in total adherent cells after treatment of HSEC with anti-ICAM-1 mAbs (6 independent experiments, t test). (D) Reduction of the frequency of transmigrating among total adherent CD4 T cells to HCMV-infected HSEC after treatment with anti-CXCL10 antibodies (before-after plot, means, and SEM are shown, paired t-test). (E) Representative phase contrast microscopy of CMV-specific effector T cell clones adherent to HCMV-infected HSEC treated with mAbs against ICAM-1 (top). Quantification of adherent and migrating CMV-specific effector CD4 T cell clones on mock-infected and HCMV-infected HSEC (7 independent experiments, t test) and its inhibition by monoclonal antibodies against ICAM-1 (2-15 independent experiments, t test of total adherent cells) are shown. (F) Quantification of adherent and migrating polyclonal regulatory CD4 T cells on HCMV-infected HSEC and after treatment of HSEC with anti-ICAM-1 or T cells with anti-CXCR3 (6 independent experiments, t test).

Figure 4: CMV-infected HSEC recruit activated effector memory CD4 T cells

(A) Schematic illustration of the two static ETM models employed as described in the Materials and Methods section. (B) Frequency of T cell subsets among CD3 T cells that have migrated into collagen (left panel) or across the transwell (right panel) using mock-infected, cytokine-treated, or HCMV-infected HSEC compared to the starting population. In transwell models CD56 staining was not performed, thus NKT cells are not indicated (4-8 independent experiments). (C) Percentage of chemokine receptor expressing T cells and (D) median FI of CD2, CD11a, and CD18 in the starting population and after migration through cytokine-stimulated or HCMV-infected HSEC in the transwell model (boxplots from 4 and mean+SEM from 3 independent experiments). (E) Representative expression of CD62L and CD45RO on CD4 T cells before ETM (left), after adherence to HCMV-infected HSEC (top right) and after migration across HCMV-infected HSEC into collagen (bottom right). (F) Fractions of central ($CCR7^+CD62L^+$; light grey) and effector ($CCR7^-/CD62L^-$; dark grey) CD4 memory T cells before and after migration through mock-infected, cytokine-treated, or HCMV-infected HSEC into collagen (8-9 independent experiments, Dunnett's post hoc test comparing fractions of T_{EM}).

Figure 5: Allogeneic T cells demonstrate Th1 activation after migration across HCMV-infected HSEC

(A) Representative plots of activation marker expression on isolated CD4 memory T cells left untreated without endothelial contact (ctrl) and 24 hours after migration through HCMV-infected or mock-infected HSEC into collagen. (B) Fractions of surface marker-positive CD4 memory T cells within CD4 T cells before and after migration through HCMV-infected or mock-infected HSEC (5-16 independent experiments, Dunnett's post hoc test). (C) Representative plots of CD69 expression versus intracellular cytokine staining of CD4 memory T cells after migration through

mock-infected, cytokine-stimulated and HCMV-infected HSEC into collagen. (D) Representative images of nitrocellulose membranes with spotted antibodies against several cytokines (bottom) and densitometric quantification as normalized mean pixel density of chemiluminescence of those cytokines (top) in supernatants from CD4 memory T cells after migration through HCMV-infected HSEC into collagen. Retrieved T cells either remained unstimulated or were treated with PMA/ionomycin before analysis. (E) Waterfall plot of more than two-fold regulated genes in CD4 memory T cells following ETM across HCMV-infected HSEC compared to the starting population as determined by real-time RT PCR array. (F) Left: Expression of CD69 on CD4 memory T cells remains unchanged when memory T cells are separated from HCMV-infected HSEC by transwell membranes with 0.3 µm pores. Right: Significant change in relative surface expression of CD69 on CD4 memory T cells after incubation of HCMV-infected HSEC with functional Abs against LFA-3 but not with blocking Abs against MHC class II, ICAM-1, CXCL10, TLR2 or EPCR or with JAK inhibitor I or methyl beta cyclodextrin (MBCD) in comparison to untreated HCMV-infected HSEC (3-11 independent experiments, one-sample t-test)

Figure 6: CMV-infected human sinusoidal endothelial cells recruit functional regulatory T cells

(A) Representative plot showing propidium iodide (PI) and annexin V staining CD4 memory T cells 72 hours after migration through mock-infected or HCMV-infected HSEC into collagen showing unchanged levels of early and late apoptosis. (B) Representative density plot of CD127 and CD25 and histogram plot of intracellular FoxP3 expression in memory CD4 T cells that migrated across HCMV-infected HSEC showing highest expression of FoxP3 in the $CD25^{hi}CD127^{lo}$ population (IMC: grey). (C) Time-dependent increase of the percentage of $CD25^{hi}$ and $CD25^{lo}$-

expressing CD4 memory T cells after migration across mock-infected or HCMV-infected HSEC into collagen compared to the pre-migratory population. (D) Frequency of $CD25^{hi}CD127^{lo}$ cells among CD4 T cells before and after migration through cytokine-stimulated or HCMV-infected HSEC in the transwell model (4 independent experiments; Dunnett's post hoc test; mean percentage of $FoxP3^{+}$ as black inserts). (E) Effector CD4 T cell proliferation as representative plots and quantified after stimulation with CD2/CD3/CD28 beads and co-incubated with CD4 memory T cells that migrated across cytokine-stimulated, mock-infected, or HCMV-infected HSEC in different ratios of effector cells to migrated cells (1:1 to 1:4) (3 independent experiments, t-test). T cells that have not migrated across HSEC are shown as a control (start).

Figure 7. Schematic representation of T cell recruitment across HCMV-infected sinusoidal endothelium

(A) HCMV infection of HSEC results in upregulated ICAM-1 expression and release of type-I interferons and interferon-regulated chemokines. (B) Allogeneic effector memory CD4 T cells and suppressive regulatory T cells predominantly migrate across HCMV-infected endothelium in an LFA-1/ICAM-1 and CXCR3/CXCL10-dependent manner. Recruited effector T cells show an activated Th1 Phenotype, which is in part mediated by the interaction of CD2 with LFA-3. Proposed consequences of the differential T cell recruitment into the liver and the additional impact of immunosuppression are indicated in italic font.

Figure 1

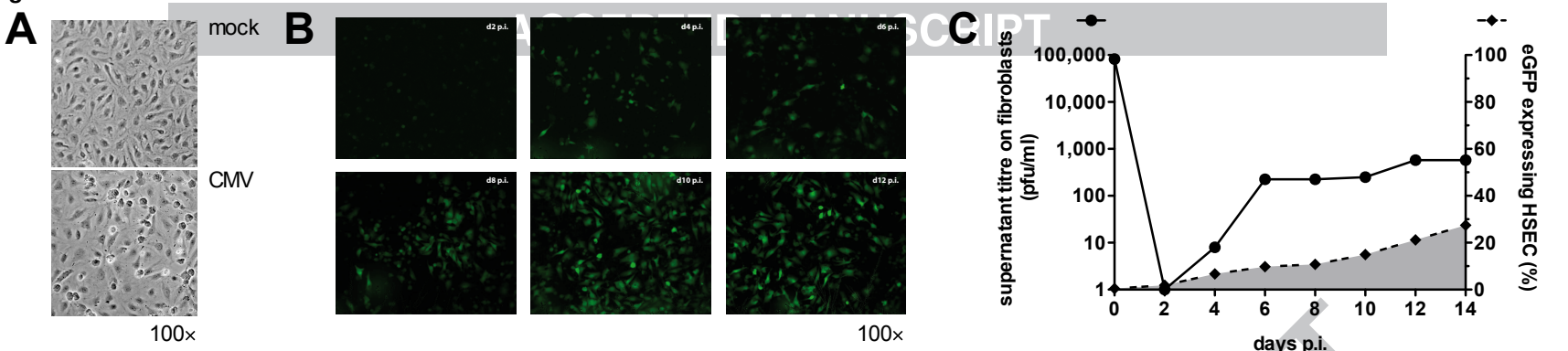
A
mock
CMV
100×
B
d2 p.i.
d4 p.i.
d6 p.i.
d8 p.i.
d10 p.i.
d12 p.i.
100×
C
supernatant titre on fibroblasts (pfu/ml)
100,000
10,000
1,000
100
10
1
0
2
4
6
8
10
12
14
days p.i.
eGFP expressing HSEC (%)
100
80
60
40
20
0

Figure 2

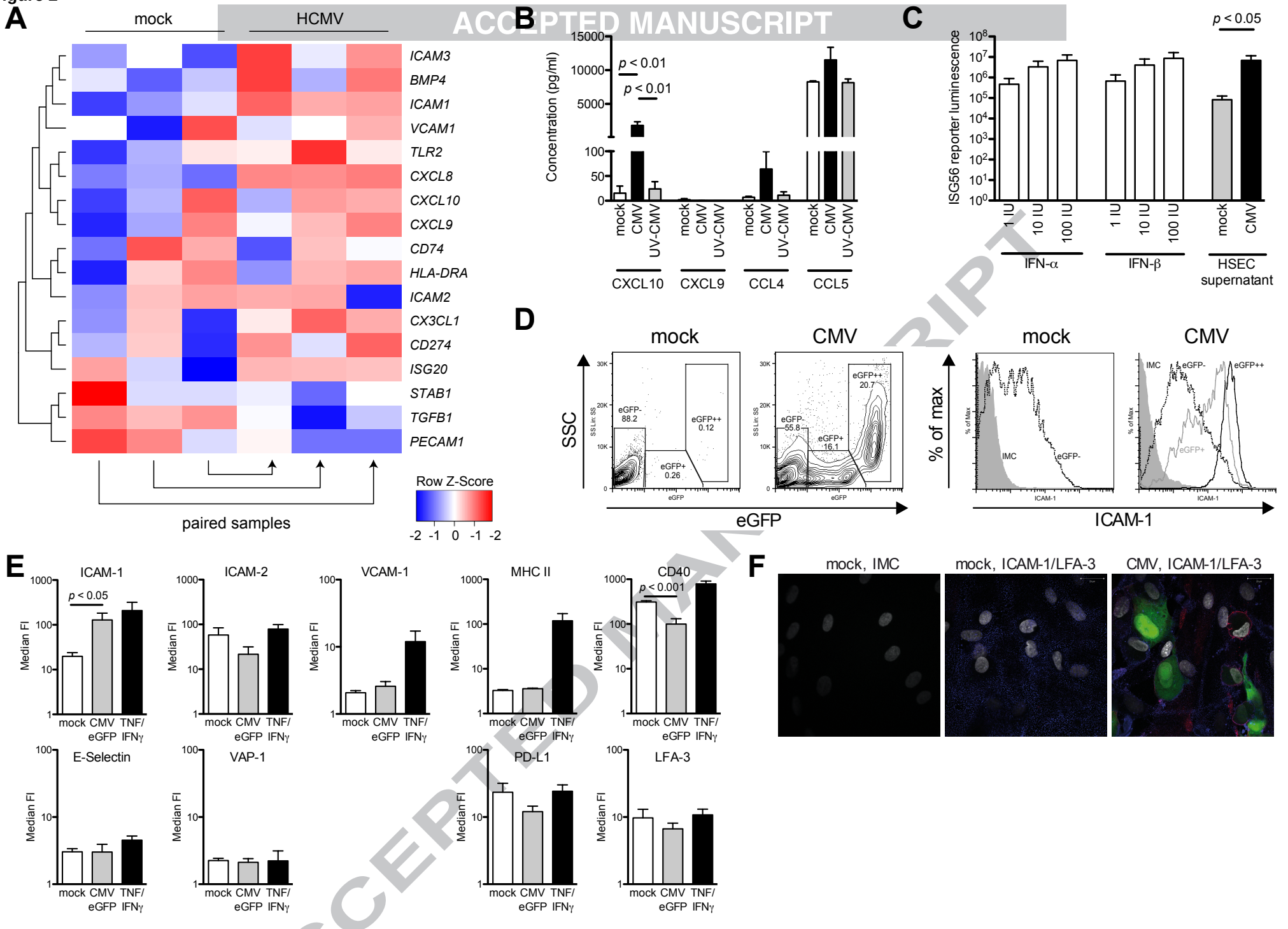

Figure 3

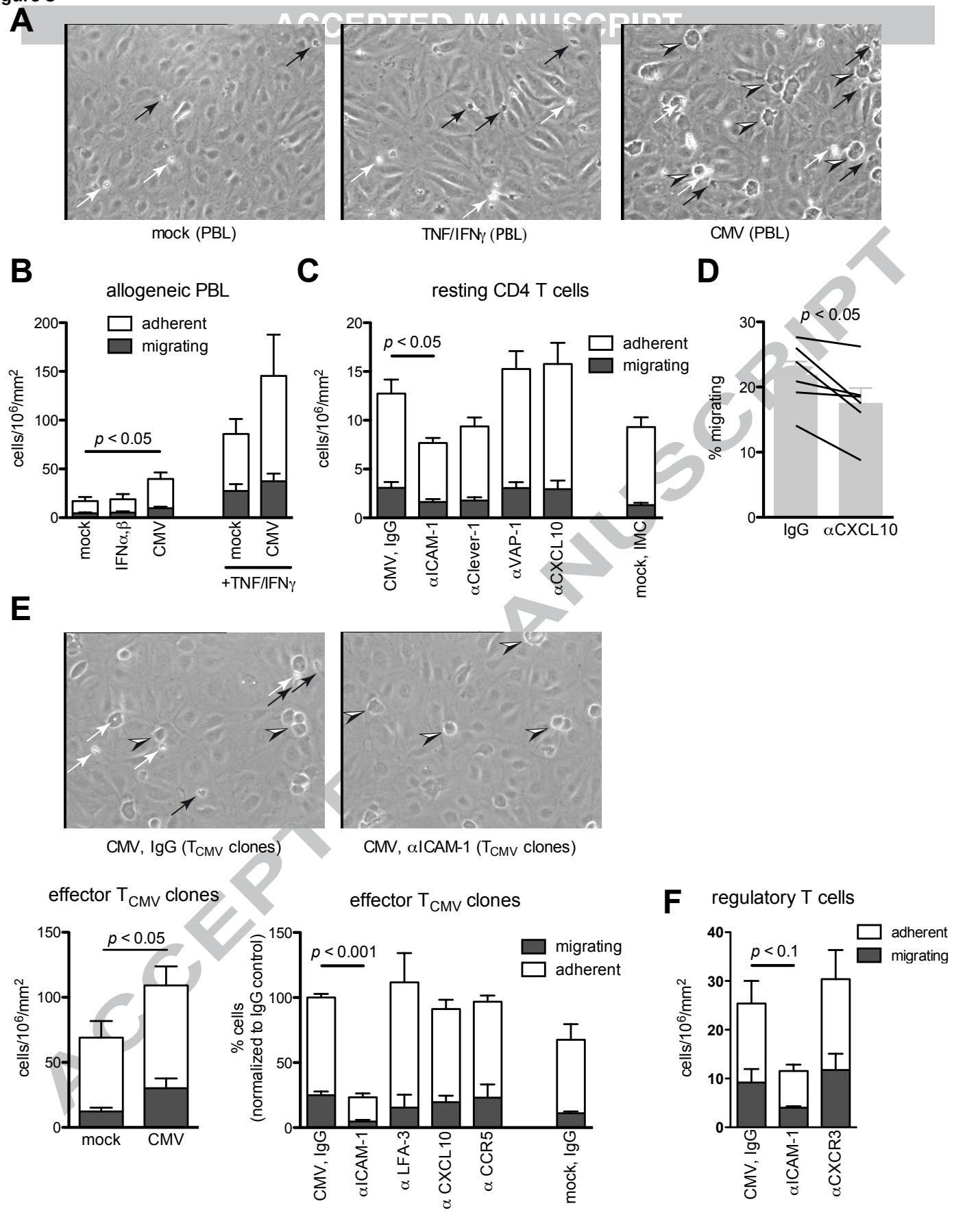

Figure 4

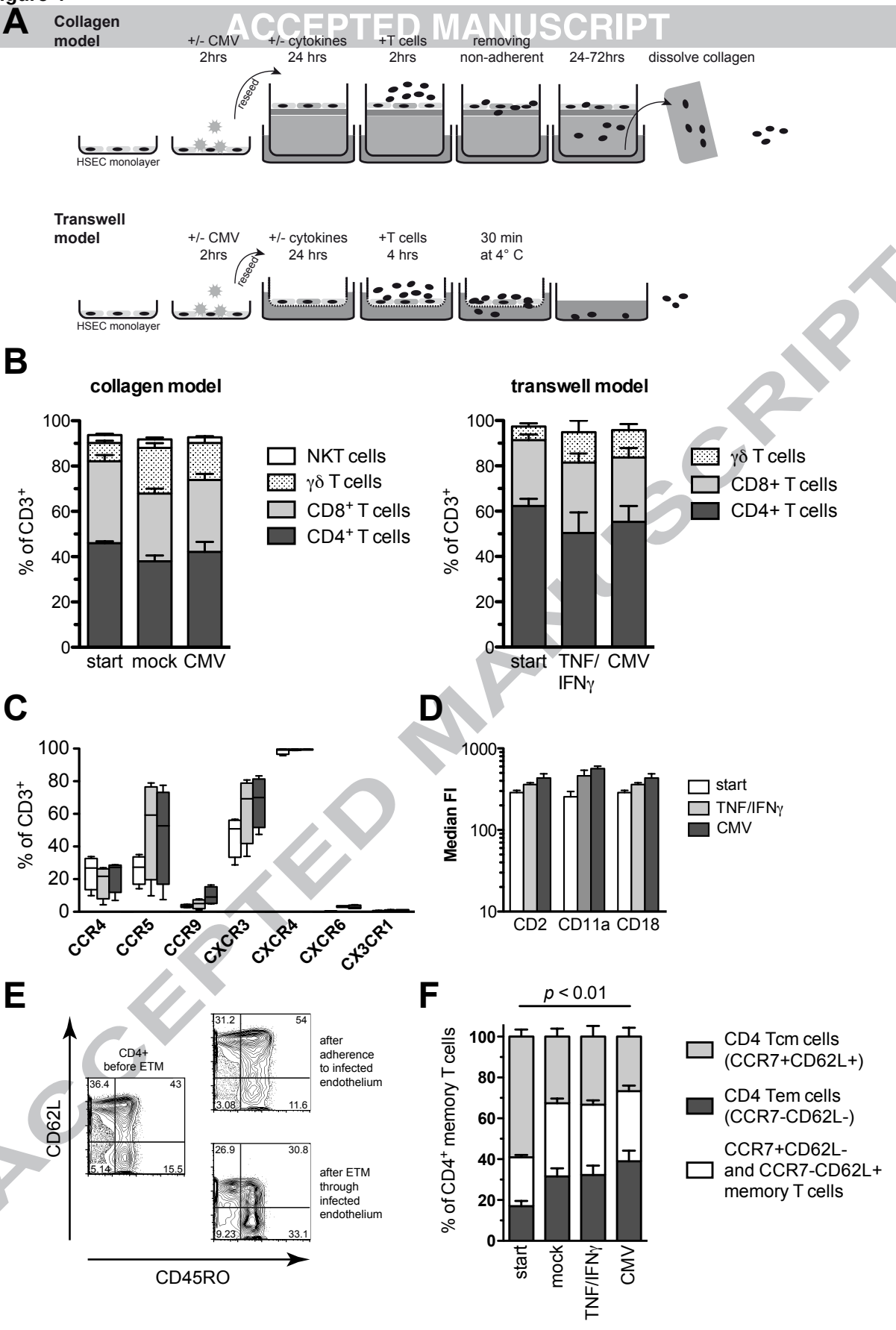

Figure 5

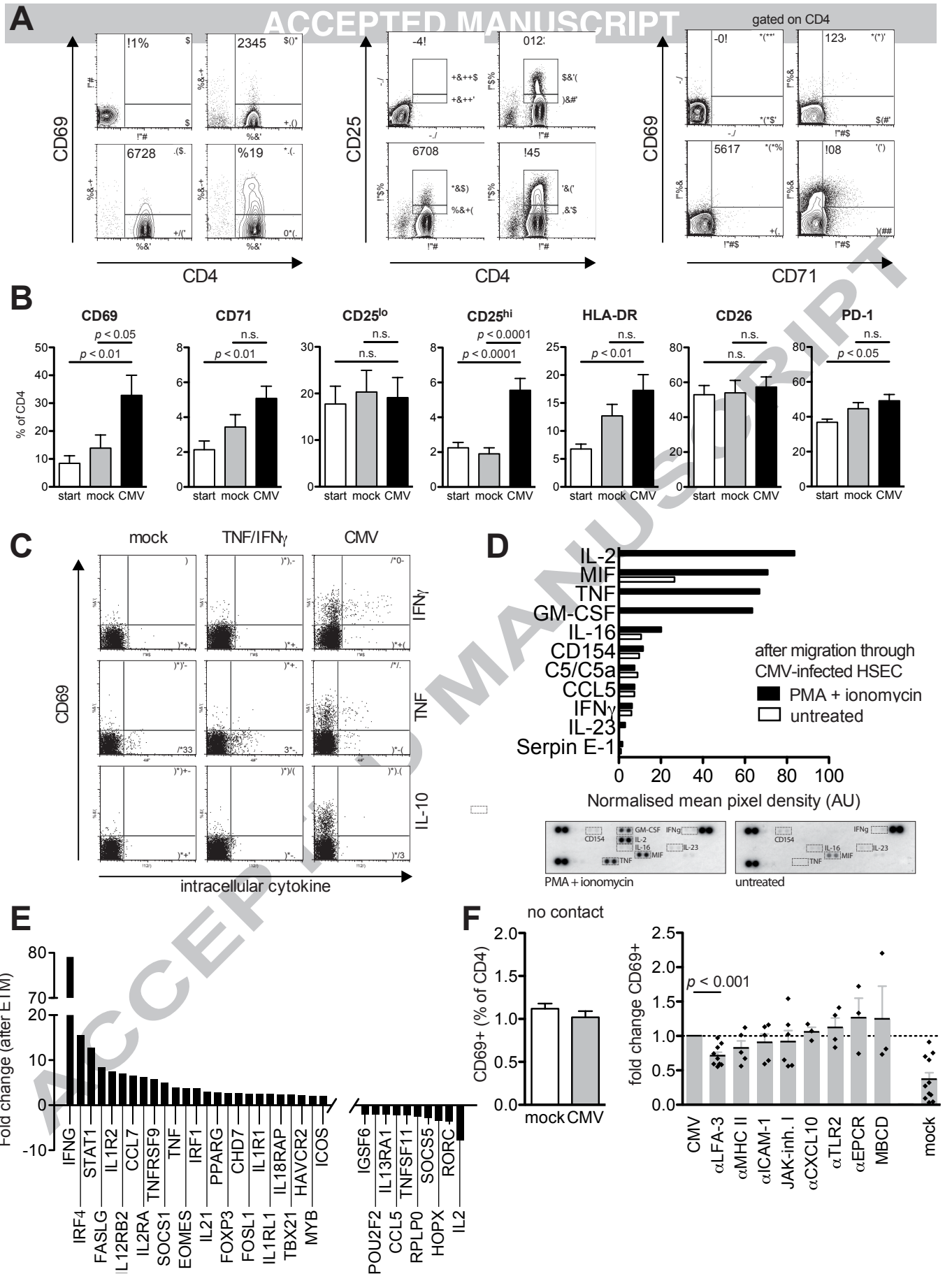

Figure 6

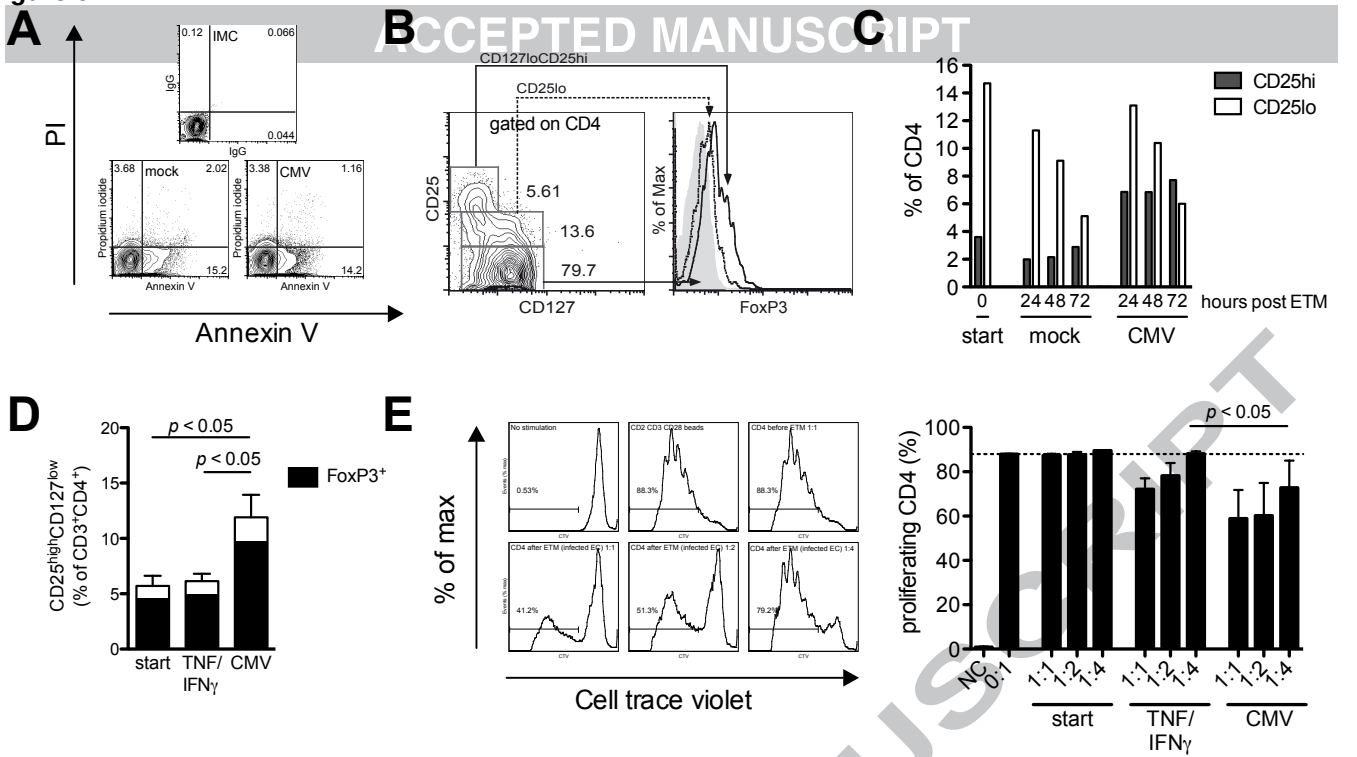

Figure 7